

Estimating a modified Grubb's exponent in healthy human brains with near infrared spectroscopy and transcranial Doppler

Terence S Leung¹, Ilias Tachtsidis¹, Martin M Tisdall²,
Caroline Pritchard², Martin Smith² and Clare E Elwell¹

¹ Department of Medical Physics and Bioengineering, University College London, London, UK

² Department of Neurocritical Care, The National Hospital for Neurology and Neurosurgery, Queen Square, London, UK

Received 13 May 2008, accepted for publication 28 October 2008

Published 27 November 2008

Online at stacks.iop.org/PM/30/1

Abstract

The relationship between cerebral blood volume (CBV) and flow (CBF) has been widely studied. One of the most significant early studies was by Grubb *et al* (1974 *Stroke* **5** 630–9), who conducted hypercapnia studies in primates with positron emission tomography (PET) and empirically found $CBV = 0.8 CBF^{0.38}$. The exponent used here has since been known as the Grubb's exponent. In this paper, we define a similar exponent known as the modified Grubb's exponent, G' , which is based on CBV and cerebral blood flow velocity (CBFV) estimated by near infrared spectroscopy (NIRS) and transcranial Doppler respectively, i.e. $G' = \log(CBV/CBV_0)/\log(CBFV/CBFV_0)$, where CBV_0 and $CBFV_0$ are baseline values. The aim of this study was to estimate the nominal value of the modified Grubb's exponent in healthy human brains. We conducted hypercapnia and hypocapnia studies on 14 healthy adult subjects. The correlation coefficient between $\log(CBV/CBV_0)$ and $\log(CBFV/CBFV_0)$ is 0.71 ($p < 0.0001$). We found a modified Grubb's exponent of 0.13 (the 95% confidence bounds are 0.10 and 0.17) which is expectedly lower than the conventional Grubb's exponents estimated by other techniques. The modified Grubb's exponent is a simple measure to quantify the hemodynamics between local CBV and global CBFV in the brain and as such may provide insight on brain physiology. Both NIRS and transcranial Doppler techniques are non-invasive and portable, facilitating future studies in other population groups such as brain-injured patients.

Keywords: Grubb's exponent, near infrared spectroscopy, transcranial Doppler, cerebral blood flow, cerebral blood volume

(Some figures in this article are in colour only in the electronic version)

Introduction

Grubb *et al* (1974) investigated the relationship between CBF and CBV in 23 primates using positron emission tomography (PET). In each primate, the arterial carbon dioxide pressure (PaCO_2) was lowered by hyperventilation and raised by hypoventilation so that the cerebral vascular resistance and hence CBF were changed. Using linear regression on a log scale, it was found that the relationship between CBF and CBV can be sufficiently quantified by a simple power law equation: $\text{CBV} = 0.8 \text{ CBF}^{0.38}$. The exponent here, in this case 0.38, has since been known as the Grubb's exponent.

Since then, similar studies have reported slightly different Grubb's exponents using different measurement techniques in animals and humans, ranging from 0.18 to 0.40 (Grubb *et al* 1974, Lee *et al* 2001, Ito *et al* 2003, Mandeville *et al* 1999, Jones *et al* 2001, Cheung *et al* 2001). Grubb's exponent has been measured mainly in two ways, namely the steady state and the dynamic state. In the steady state, the CBF and CBV have settled to steady values after a physiological challenge such as hypercapnia or hypocapnia (Grubb *et al* 1974, Lee *et al* 2001, Ito *et al* 2003, Cheung *et al* 2001). As for the dynamic state, the Grubb's exponent was often measured in neural stimulation studies in which both CBF and CBV were still changing following stimulation such as electrical stimulations (Mandeville *et al* 1999, Jones *et al* 2001).

At first sight, Grubb's exponent seems to lack some degree of mathematical rigor. Considering the general formulation of Grubb's exponent that $\text{CBV} = A \times \text{CBF}^G$, where A is a dimensionless constant, and G is the Grubb's exponent, it is immediately clear that the units of CBV ($\text{ml}/100 \text{ g}$) and CBF ($\text{ml}/100 \text{ g min}^{-1}$) are different and the formulation has no obvious physical meaning. The formulation is in fact best considered as a regression equation as it was originally intended, in which a linear relationship was found between two variables. In this case, they are $\log(\text{CBV})$ and $\log(\text{CBF})$, and the formulation becomes $\log(\text{CBV}) = G \times \log(\text{CBF}) + \log(A)$.

The formulation of Grubb's exponent is often expressed as a proportional change, i.e.

$$(\text{CBV}/\text{CBV}_0) = (\text{CBF}/\text{CBF}_0)^G$$

or

$$G = \frac{\log(\text{CBV}/\text{CBV}_0)}{\log(\text{CBF}/\text{CBF}_0)}, \quad (1)$$

where CBV_0 and CBF_0 are the baseline values of CBV and CBF (Buxton and Frank 1997, Mandeville *et al* 1999, Friston *et al* 2000, Wu *et al* 2002, Boas *et al* 2003, Culver *et al* 2003, Kong *et al* 2004, Zheng *et al* 2005, Franceschini *et al* 2007). The advantage of this expression is that the units of CBV and CBF, and the constant A have been cancelled out, and the whole equation becomes dimensionless, which circumvents the issue of unit mismatch in CBV and CBF. More importantly, equation (1) is compatible with the steady state of the windkessel model (Mandeville *et al* 1999) and the balloon model (Buxton and Frank 1997, Buxton *et al* 1998) which gives this proportional expression a physical meaning. Both models have been developed to explain the dynamic relationship between CBV and CBF during neural stimulation of the brain. Equation (1) is also compatible with variants of these two models (Friston *et al* 2000, Kong *et al* 2004, Zheng *et al* 2005). According to the windkessel model, the Grubb's exponent is always smaller than 0.5 for laminar flow through a compliant and passively reacting compartment (Mandeville *et al* 1999).

It is worth mentioning that the formulation of Grubb's exponent may not match the general expectation of the behaviour of CBV and CBF in certain conditions. For example, when blood ceases to flow in the brain ($\text{CBF} = 0$), it is expected that blood still resides in the

brain ($CBV \neq 0$). In contrast, equation (1) predicts a zero CBV in such circumstances. This seemingly problematic situation can be explained by considering equation (1) in the context of the balloon model mentioned earlier. The balloon considered here has one inlet and one outlet. It is elastic and collapsed completely when there is neither inflow nor outflow of blood ($CBF = 0$), which means that the balloon cannot contain any blood, and therefore the blood volume is zero ($CBV = 0$). In reality, blood vessels will not collapse completely when there is no blood flow, and equation (1) is therefore not applicable in the absence of blood flow.

There are a number of ways to measure CBV and CBF, namely, PET (Grubb *et al* 1974, Ito *et al* 2003), magnetic resonance imaging (MRI) (Lee *et al* 2001, Wu *et al* 2002), and dynamic computed tomography (CT) (Cenic *et al* 1999). While Mandeville *et al* (1999) employed MRI to measure CBV and laser Doppler flowmetry to measure CBF, several studies adopted an 'all optical' approach to measure both CBV and CBF using optical techniques such as NIRS (Jones *et al* 2001, Cheung *et al* 2001), diffuse optical tomography (Culver *et al* 2003), laser Doppler flowmetry (Jones *et al* 2001) and correlation spectroscopy (Cheung *et al* 2001, Culver *et al* 2003). Although both laser Doppler flowmetry and correlation spectroscopy are based on the interaction between photons and moving red blood cells to measure blood flow, their theoretical formulations are different. Apart from cerebral hemodynamic modeling, another use of the Grubb's exponent is to act as a parameter for comparison of results. When CBV and CBF are altered, and measured in a study using a particular technique, Grubb's exponent is often calculated and compared with those obtained from other studies.

Aims

The aim of this study was to estimate a 'modified' Grubb's exponent in healthy human brains using NIRS and transcranial Doppler techniques. In comparison to other imaging techniques such as PET, MRI and dynamic CT, both NIRS and transcranial Doppler are relatively simple to use and can provide bedside monitoring in patients. However, transcranial Doppler does not measure CBF in a localized region directly. Instead, it measures the cerebral blood flow velocity (CBFV) of a major supplying blood vessel which can be considered as a global measure of the blood flow in the brain. To mark such a difference in the use of CBFV rather than CBF, we refer to this new measure as the 'modified' Grubb's exponent.

One interpretation of the Grubb's exponent in equation (1) is that it is a ratio of normalized CBV to normalized CBF in a log scale. In all previous studies, the Grubb's exponent has been shown to be smaller than 1 indicating that normalized changes in CBF are always larger than those in CBV. While the conventional Grubb's exponent quantifies the relationship between localized blood volume and localized blood flow in the brain, the newly defined modified Grubb's exponent focuses on the relationship between localized blood volume and global blood flow in the brain. Subsequently, the modified Grubb's exponent can also provide a different kind of physiological information. For example, the cerebrovascular carbon dioxide (CO_2) reactivity in patients, i.e. the change in CBV, CBF or CBFV in response to hypercapnia/hypocapnia, may be different globally and locally (Vernieri *et al* 2004) which may be assessed by CBFV and CBV, respectively. The modified Grubb's exponent can then serve as a measure of localized CBV changes per unit change of global CBFV. (Both CBV and CBFV are normalized and converted to a log scale.) In situations such as localized cerebral infarction or hemorrhage where only one part of the brain is affected, local perfusion may be altered resulting in a specific region of CBV response to hypercapnia/hypocapnia. The modified Grubb's exponent described in this paper may vary over the injured and uninjured regions of the brain, and as such may provide valuable information on the patho-physiology of the brain.

This study aims to establish a nominal value for the modified Grubb's exponent in healthy human brains. We conducted a series of experiments altering the CBV, CBF and CBFV by conducting hypocapnia and hypercapnia, and then used the NIRS and transcranial Doppler measurements to determine the modified Grubb's exponent. In the future, similar studies will be carried out in brain-injured patients so that their modified Grubb's exponents can be compared with those from healthy adults obtained here. In this paper, we also discussed the validity of using CBV to predict CBF or CBFV and vice versa, once a (modified) Grubb's exponent has been derived.

Methods

Near infrared spectroscopy

NIRS is an optical technique, which relies on the reflected light through the brain to measure CBV and oxygenation (Delpy and Cope 1997). The NIRS monitor used in this study (NIRO-300, Hamamatsu Photonics KK) uses spatially resolved spectroscopy to measure tissue oxygen saturation and tissue haemoglobin index (THI) which is by definition a scaled measure of absolute CBV (Suzuki *et al* 1999). Because of the scaling factor, THI is best used as a measure of proportional changes in CBV and as such the scaling factor can be cancelled out. The cerebral tissue oxygen saturation measurement of this NIRS monitor has previously been shown to be sensitive to intracerebral oxygenation changes in the adult head (Al-Rawi *et al* 2001).

Transcranial Doppler ultrasonography

In transcranial Doppler ultrasonography, the CBFV is measured within a major artery to the brain using a non-invasive ultrasound probe positioned at the temple region of the subject (Aaslid *et al* 1982), and the ultrasound beam is often focused on the middle cerebral artery. In this paper, all CBFV values refer to those measured at the middle cerebral artery. Bishop *et al* (1986) have shown that there is a strong correlation between percentage changes in CBF (measured by xenon CT) and CBFV ($r = 0.85$, $p < 0.001$) in response to hypercapnia. Martin *et al* (1990) measured CBF using radioactive microspheres and CBFV in 14 newborn lambs while altering their CBF by infusing dopamine or saline. They found a correlation between absolute values of CBF and CBFV to be $r = 0.51$ ($p < 0.001$) and provided the following prediction equation derived from regression analysis:

$$\text{CBF} = 1.5 \text{ CBFV} + 71.4. \quad (2)$$

Despite numerous studies on the relationship between CBF and CBFV, this is the only one that provides a prediction equation.

Experiments

This study was approved by the Joint Research Ethics Committee of the National Hospital for Neurology and Neurosurgery and the Institute of Neurology. Fourteen healthy adult volunteers with median age of 31 years (range 27–39) participated in this study.

A NIRS monitor (NIRO300, Hamamatsu photonics KK) was used in this study to measure THI. This NIRS monitor has 4 wavelengths (775, 826, 850 and 909 nm). Although not used in this study, changes of oxy- and deoxy-hemoglobin concentrations can also be measured by this NIRS monitor. Two optical probes were placed on the left and right sides of the forehead, respectively. The source and detector spacing for both probes was 5 cm. The probes

were covered by a black cloth which shielded the probes from ambient light. The CBFV was measured by a 2 MHz transcranial Doppler flowmeter (Pioneer TC2020, Nicolet, UK) with the probe fixed in place over the right temporal region of each subject. A modified Boyles anaesthetic machine was used to deliver gas to the subject via a Mapelson E (Ayres *t*-piece) breathing system which was connected to a mouthpiece with the expiratory limb of 50 cm in length. The fraction of inspired oxygen (FiO_2) and the end tidal carbon dioxide ($EtCO_2$) were measured using an inline gas analyser (Hewlett Packard, UK) and a CO_2 SMO optical sensor (Novamatrix Medical Systems Inc), respectively. The $EtCO_2$ reflects the amount of carbon dioxide in the brain. An increase in $EtCO_2$ could indicate a rise in the carbon dioxide level in the brain causing vasodilation which leads to increases in CBF, CBFV and CBV. Similarly, a decrease in $EtCO_2$ could indicate a drop in the carbon dioxide level in the brain causing vasoconstriction which leads to decreases in CBF, CBFV and CBV.

In the hypocapnia experiments, the subjects hyperventilated and aimed to reduce their $EtCO_2$ by 1.5 kPa. They maintained a stable $EtCO_2$ at this reduced level for 5 min and then returned to a normal breathing rate allowing $EtCO_2$ to return to baseline values over approximately 5 min. In the hypercapnia experiments, approximately 6% CO_2 was added to the inspired gases and was titrated to induce an increase in $EtCO_2$ of 1.5 kPa. The elevated $EtCO_2$ was maintained for 10 min and the inspired carbon dioxide fraction was then returned to zero for a further 5 min.

Data analysis

Natural fluctuations exist in both the THI and CBFV signals due to physiological oscillations such as heart beats and respiration (Elwell *et al* 1999, Obrig *et al* 2000, Leung *et al* 2008). To minimize the effects of these fluctuations, 2 min worth of data were averaged for both THI and CBFV to obtain the baseline values (i.e. THI_0 and $CBFV_0$) for each dataset. To further minimize the effects of outliers, the averaging was performed using the trimmed mean which first removed the largest and smallest 5% of data points and then averaged the remaining data points. Alternatively, using a median filter should have a similar effect. For hypocapnia and hypercapnia, both THI and CBFV signals were settled to stable levels 3 min after the introduction of these challenges. The following 2 min worth of data were then averaged to obtain the mean THI and CBFV values, again using the trimmed mean approach. A typical example of all the recorded signals is shown in figure 1.

As discussed earlier, THI is a measure of CBV and from now on CBV is used instead of THI in the following text. Linear regression was performed between $\log(CBV/CBV_0)$ and $\log(CBFV/CBFV_0)$, and the gradient of the regression line is the modified Grubb's exponent, G' :

$$G' = \frac{\log(CBV/CBV_0)}{\log(CBFV/CBFV_0)}. \quad (3)$$

In an attempt to determine also the conventional Grubb's exponent, equation (2) has been used to convert CBFV into CBF. The Grubb's exponent was determined similarly with linear regression except $\log(CBF/CBF_0)$ was used this time instead of $\log(CBFV/CBFV_0)$.

Results

Table 1 shows the $EtCO_2$, THI and CBFV at baseline, and during hypercapnia in each subject, and the group mean and standard deviation. The actual increase of $EtCO_2$ during hypercapnia was different in each subject, from 1 kPa (subjects 3 and 4) to 2.3 kPa (subject 12). Table 2

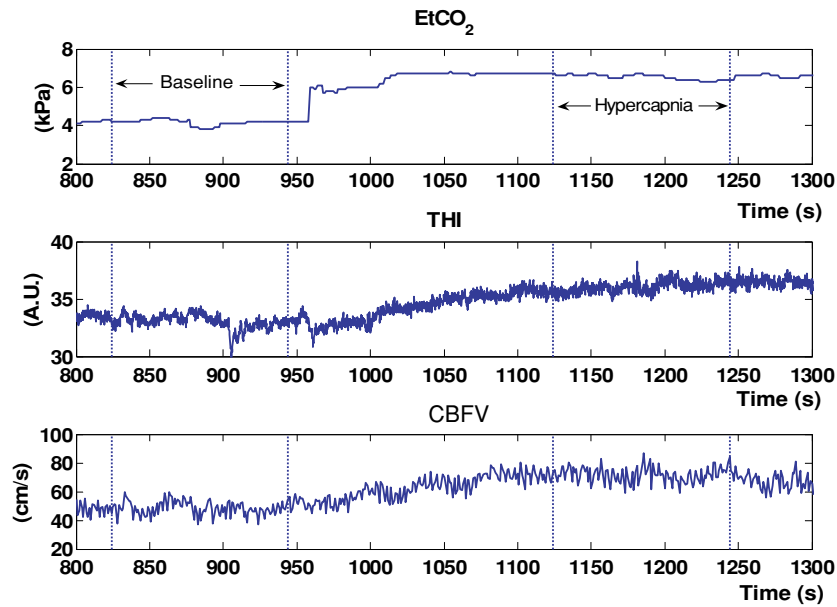


Figure 1. EtCO₂, THI and CBFV increased during hypercapnia. Vertical dotted lines mark the beginning and end points of data points (2 min) to be averaged in the analysis.

Table 1. The EtCO₂, THI and CBFV at baseline and during hypercapnia in each subject, and the group mean and standard deviation.

Subject ID	Baseline EtCO ₂ (kPa)	Hypercapnia EtCO ₂ (kPa)	Baseline THI (AU) ^a (left/right)	Hypercapnia THI (AU) (left/right)	Baseline CBFV (cm s ⁻¹)	Hypercapnia CBFV (cm s ⁻¹)
1	5.0	6.6	43.9/41.5	44.8/42.0	18.9	23.5
2	5.9	7.0	72.8/60.9	73.7/57.2	38.6	41.3
3	5.9	6.9	62.8/48.3	62.7/48.0	38.6	40.8
4	6.0	7.0	56.5/47.2	57.7/47.7	55.9	56.5
5	6.0	7.3	51.4/51.3	50.0/48.2	60.8	63.5
6	5.3	7.1	46.6/24.0	49.6/25.2	55.1	62.6
7	5.8	7.1	35.6/46.4	34.1/46.6	41.5	45.0
8	5.2	6.4	47.3/86.5	50.8/90.1	34.0	39.1
9	5.2	6.6	100.3/31.2	98.2/30.2	30.7	30.1
10	4.3	6.2	42.5/46.1	44.4/49.2	46.2	69.8
11	5.1	6.9	76.4/30.8	76.9/31.8	48.5	51.1
12	4.2	6.5	33.1/25.2	36.1/26.6	48.3	71.7
13	5.6	7.4	43.0/47.9	45.5/48.6	51.7	60.5
14	5.4	6.6	25.3/21.1	26.4/22.3	64.7	72.0
Mean ± std	5.4 ± 0.6	6.8 ± 0.4	52.7 ± 19.8/ 43.5 ± 17.1	53.6 ± 19.1/ 43.8 ± 17.3	45.3 ± 12.5	52.0 ± 15.7

^a AU: arbitrary unit.

shows similar results for hypocapnia. The actual decrease of EtCO₂ during hypocapnia was also different in each subject, from 1.3 kPa (subject 12) to 2.3 kPa (subject 1).

In each subject, two series of THI measurements were obtained, i.e. one from the NIRS probe placed on the left side of the forehead and one from the right. It can be seen from

Table 2. The EtCO₂, THI and CBFV at baseline and during hypocapnia in each subject and the group mean and standard deviation.

Subject ID	Baseline EtCO ₂ (kPa)	Hypocapnia EtCO ₂ (kPa)	Baseline THI (AU) ^a (left/right)	Hypocapnia THI (AU) (left/right)	Baseline CBFV (cm s ⁻¹)	Hypocapnia CBFV (cm s ⁻¹)
1	5.8	3.5	45.6/42.8	43.9/41.9	19.8	13.2
2	5.8	4.0	74.3/65.1	70.1/60.4	31.9	22.3
3	6.0	4.2	65.0/49.2	61.4/48.4	36.2	26.2
4	5.8	4.0	56.4/47.9	55.1/45.7	49.8	37.6
5	6.0	4.0	52.3/53.9	50.6/49.5	55.4	45.6
6	5.8	4.1	46.5/25.1	45.8/23.5	49.1	39.1
7	5.9	4.4	34.1/46.7	35.1/45.3	37.7	26.2
8	5.3	3.2	48.7/91.0	45.7/86.1	31.8	20.4
9	5.3	3.9	104/30.9	97.7/30.4	28.9	19.0
10	4.8	3.0	41.9/48.3	41.9/45.3	52.0	37.3
11	5.8	4.0	76.7/31.2	74.6/31.0	45.3	30.7
12	4.5	3.2	33.6/26.0	32.8/25.1	46.6	37.3
13	5.9	4.1	44.2/53.7	41.5/47.2	51.5	38.0
14	5.5	3.7	25.3/21.7	24.7/20.8	59.9	45.0
Mean ± std	5.6 ± 0.5	3.8 ± 0.4	53.5 ± 20.7/ 45.3 ± 18.4	51.5 ± 19.2/ 42.9 ± 17.0	42.6 ± 11.6	31.3 ± 10.2

^a AU: arbitrary unit.

table 1 that in certain subjects the THI on both sides of the forehead can be quite different, e.g. in subject 9, the baseline THI on the left side is 100.3 AU (arbitrary unit) while that on the right is 31.2 AU. It is worth providing more details over such a large discrepancy here. Spatially resolved spectroscopy is based on the difference of optical attenuation measured by two closely spaced detectors. In general, the higher the underlying blood volume, the larger the attenuation difference. Occasionally, a blood vessel may exist at a closer proximity to one of the detectors and causes a bias. This is likely to be the cause of such a large discrepancy of THI between both sides of the forehead observed here. However, despite the difference in the baseline values, it is expected that their proportional changes will still be similar. This is the reason why THI is often used as a relative rather than an absolute measure. This once again reiterates the fact that THI is best used as percentage changes from a baseline value, rather than an individual value for comparison.

Figure 2 depicts the scatter plot of $\log(\text{CBV}/\text{CBV}_0)$ and $\log(\text{CBFV}/\text{CBFV}_0)$ for the 14 subjects. The distribution of the data points is consistent with the general understanding of CBV and CBFV during hypercapnia and hypocapnia, i.e. both CBV and CBFV tend to increase during hypercapnia because of vasodilation while they tend to decrease during hypocapnia due to vasoconstriction. It is noted that the four data points on the rightmost of figure 2 correspond to the two subjects who had the largest increases in EtCO₂ during hypercapnia, i.e. subjects 10 and 12.

Table 3 shows the resulting modified Grubb's exponents and their 95% confidence bounds using CBV measurements collected from the left, the right and both sides of the forehead. The three estimates of the modified Grubb's exponent are essentially the same. The regression line in figure 2 was derived using CBV measurements from both sides of the forehead. Figure 2 also shows the 95% confidence interval (inner dotted lines) and the 95% prediction interval (outer dotted lines) (Dawson-Saunders and Trapp 1994). The correlation coefficient is 0.71 ($p < 0.0001$), and the modified Grubb's exponent is 0.13. The regression line crosses

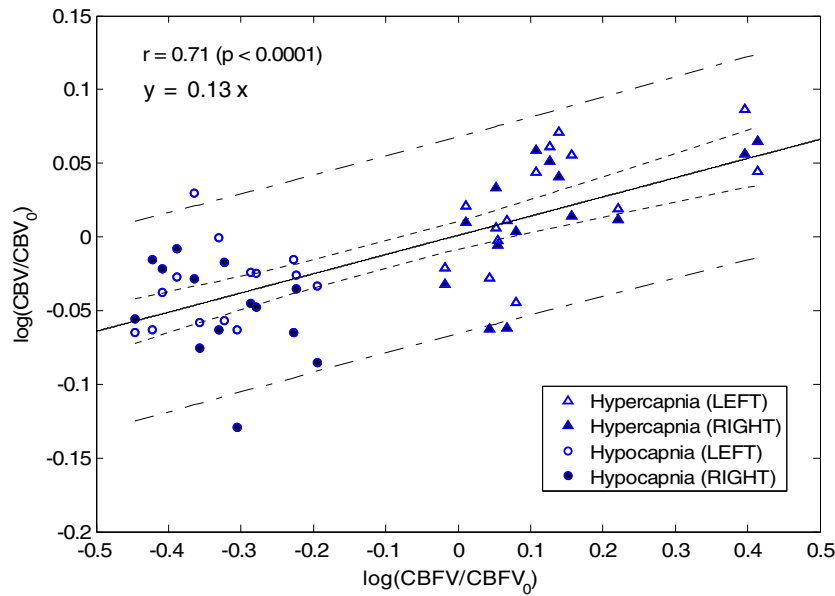


Figure 2. Scatter plot and the linear regression between $\log(\text{CBV}/\text{CBV}_0)$ and $\log(\text{CBFV}/\text{CBFV}_0)$ during hypercapnia and hypocapnia. The outer and inner dotted lines are the prediction and confidence intervals of the regression line, respectively.

Table 3. Modified Grubb's exponents estimated by CBFV measured using transcranial Doppler and CBV measured using NIRS with the probe positioned at the left, right and both sides of the human forehead.

Data sets	Modified Grubb's exponent (95% confidence bounds)
CBV at the left side of the forehead	0.13 (0.09 and 0.18)
CBV at the right side of the forehead	0.13 (0.07 and 0.19)
CBV at both left and right sides of the forehead	0.13 (0.10 and 0.17)

the zero coordinate, i.e. the y -intercept = 0 because both CBV and CBFV measurements have been normalized by their baseline values which correspond to $\log(1) = 0$.

The use of equation (2) to convert CBFV into CBF led to a Grubb's exponent of 0.30 (95% confidence bounds are 0.23 and 0.38) and a correlation coefficient of 0.74 ($p < 0.0001$) using the converted CBF and CBV measurements from both sides of the forehead.

Discussion and conclusion

Application of the modified Grubb's exponent

The physiological relationship between CBV and CBF is complex. It depends on many physiological factors such as the arteriole resistance, arterial/venous/capillary compartment volume ratio and venous compliance among others (Mandeville *et al* 1999). The Grubb's exponent is one way to provide a simple quantitative measure of the haemodynamics between CBV and CBF in a population. In this paper, we introduced a similar measure for CBV and

Table 4. Grubb's exponents found in previous studies.

Studies	Methods	Subjects	States	Grubb's exponent
Mandeville <i>et al</i> (1999)	MRI and laser Doppler flowmetry ^a	Rats, $n = 3$	Dynamic	0.18
Jones <i>et al</i> (2001)	Optical imaging and laser Doppler flowmetry ^a	Rats, $n = 10$	Dynamic	0.29
Grubb <i>et al</i> (1974)	PET	Primates, $n = 23$	Steady	0.38
Lee <i>et al</i> (2001)	MRI	Rats, $n = 6$	Steady	0.40
Jones <i>et al</i> (2001)	Optical imaging and laser Doppler flowmetry ^a	Rats, $n = 10$	Steady	0.31
Cheung <i>et al</i> (2001)	Optical imaging and correlation spectroscopy ^a	Rats, $n = 16$	Steady	0.23
Culver <i>et al</i> (2003)	Optical imaging and correlation spectroscopy ^a	Rats, $n = 5$	Steady	0.03 ^b
Ito <i>et al</i> (2003)	PET	Humans, $n = 9$	Steady	0.29
Leung <i>et al</i> (this work)	Optical technique and transcranial Doppler	Humans, $n = 14$	Steady	0.30 ^c

^a Although both laser Doppler flowmetry and correlation spectroscopy are based on the interaction between photons and moving red blood cells, their theoretical formulations are different.

^b All steady state studies shown here are based on hypercapnia/hypocapnia except the one by Culver *et al* (2003) which was conducted with ischemia in rats and hence a very different Grubb's exponent from those obtained by other studies.

^c In this paper, a *modified* Grubb's exponent of 0.13 has been found. By applying equation (2) and the same estimation technique described here, a Grubb's exponent of 0.30 has been obtained.

CBFV known as the modified Grubb's exponent. While the measurement of Grubb's exponent in humans requires imaging techniques such as PET, fMRI or dynamic CT, the measurement of the modified Grubb's exponent can be performed using simpler and bedside techniques such as transcranial Doppler and NIRS. One advantage of using NIRS is that apart from CBV, the technique can also provide oxygenation information, which although not used in this study, could provide additional insights in brain physiology. The simultaneous use of transcranial Doppler and NIRS to measure CBFV, CBV and cerebral oxygenation has been previously attempted in a study which found the measurements provide useful information about both hemodynamic and metabolic cerebral adaptive status in patients with occlusive disease in a simple, non-invasive and reliable way (Vernieri *et al* 2004).

In this paper, we estimated a nominal value of 0.13 for the modified Grubb's exponent in 14 healthy adults. It is expected that this value may be different in patients with localized cerebral infarction, hemorrhage or other types of brain injuries or pathologies. Multichannel NIRS systems (optical topography) are now available commercially which can measure regional CBV and oxygenation changes (Koizumi *et al* 2003). With a multichannel NIRS system, it can be envisaged that experiments can be performed to estimate the regional modified Grubb's exponents over different parts of the head of a brain-injured patient which could provide useful information about the hemodynamics of an injured brain. The resulting modified Grubb's exponent can also be used in the mathematical modeling of cerebral haemodynamics in these pathological conditions.

Comparison between the conventional and modified Grubb's exponents

It is generally believed that changes in CBF will follow those in CBFV as long as the cross-sectional area of the vessel targeted by the transcranial Doppler remains constant during the measurement, and various studies showed that this is indeed the case in healthy subjects

during hypercapnia (Panerai 1998). CBF and CBFV however have different baseline values. Therefore, although their changes might be correlated during hypercapnia, the actual values of percentage changes are different. This is the reason why the typical value of the modified Grubb's exponent is expected to be different from that of the conventional Grubb's exponent. Table 4 lists a number of previous studies on the measurements of CBV and CBF using various measuring techniques and the Grubb's exponents found. In comparison, the modified Grubb's exponent found here was smaller in value. This is in fact expected because previous studies have shown that the percentage change in CBFV is larger than that in CBF during hypercapnia measured using transcranial Doppler and Xenon CT (Bishop *et al* 1986, Ulrich *et al* 1995). In other words, a larger value of CBFV (versus CBF) is expected in the denominator of the modified Grubb's exponent as shown in equation (3), resulting in a smaller modified Grubb's exponent (versus the conventional Grubb's exponent). In the case of patients, it has been pointed out that CBFV and CBF may vary differently with intracranial pathology (Brauer *et al* 1998, Pindzola *et al* 2001), and therefore the modified Grubb's exponent can offer a different perspective on cerebral hemodynamics compared to the conventional Grubb's exponent.

Most of the studies shown in table 4 were carried out in animals except one study (Ito *et al* 2003) which found a Grubb's exponent of 0.29 in nine human subjects. Equation (2) has been derived from an animal study, and strictly speaking, it is not appropriate to use it in the human study here. Despite this concern, it is interesting to see that if we apply this equation to convert CBFV into CBF, we would theoretically be able to derive a (conventional) Grubb's exponent. Using this approach and the same data, a Grubb's exponent of 0.30 (included in table 4) has been obtained which is similar in value to those found by other studies, especially the Ito study (Ito *et al* 2003), and could provide evidence that equation (2) may also be valid in humans. Also, the 95% confidence bounds of this Grubb's exponent (0.23 and 0.38) are within the range of those previously reported as shown in table 4.

Predicting CBV with CBFV measurement

One may wonder whether it is appropriate to use equation (3) as a predictive equation to predict CBV from CBFV using the modified Grubb's exponent (0.13) found in this study. The scattering of the data points on figure 2 is large but not atypical of this kind of study. As shown in figure 2, a wide prediction interval (outer dotted lines) exists for the regression line indicating that the prediction of relative CBV using a single measurement of relative CBFV will result in a large uncertainty. In other words, it is not appropriate to use the modified Grubb's exponent formulation to predict CBV based on a CBFV measurement on an individual basis. The confidence interval (inner dotted lines) of the regression line is narrower showing that predicting relative CBV using the mean of relative CBFV in a population would provide a higher certainty.

Predicting CBF/CBFV with CBV measurement

In some studies, the Grubb's exponent was inverted and used to predict relative CBF based on relative CBV, i.e.

$$(CBF/CBF_0) = (CBV/CBV_0)^\beta$$

or

$$\log(CBF/CBF_0) = \beta \times \log(CBV/CBV_0), \quad (4)$$

where $\beta = 1/G$ (Franceschini *et al* 2007). For NIRS, this approach has a particular advantage because CBV is often easier to measure than CBF. In particular, if CBF can be predicted from

CBV measurements, the cerebral metabolic rate of oxygen can also be derived. Although equation (4) seems algebraically consistent with equation (1), there is a subtle problem to use equation (4) for prediction. In the original regression analysis based on equation (1), the independent variable is $\log(\text{CBF}/\text{CBF}_0)$ and the dependent variable is $\log(\text{CBV}/\text{CBV}_0)$. In other words, the Grubb's exponent found is only supposed to be valid for predicting CBV/CBV_0 based on CBF/CBF_0 but not vice versa. (It is noted that both CBF and CBV changes are a consequence of CO_2 changes and in this sense both CBV and CBF are dependent variables. However, for the sake of linear regression, one variable is always defined as the independent variable, i.e. in this case CBF, while the other one as dependent variable, i.e. CBV.) All the studies listed in table 4 were based on equation (1) in the estimation of the Grubb's exponents, G . If they were to use instead $\log(\text{CBV}/\text{CBV}_0)$ as the independent variable and $\log(\text{CBF}/\text{CBF}_0)$ the dependent variable in the regression analysis, i.e. equation (4), they would have obtained a β which would not be equal to $1/G$. This is because the variances in $\log(\text{CBF}/\text{CBF}_0)$ and $\log(\text{CBV}/\text{CBV}_0)$ measurements would have been different. In summary, it is not strictly appropriate to use any values of the Grubb's exponent listed in table 4 to predict CBF based on CBV measurements. The more conventional use of the Grubb's exponent in the current literature is in the mathematical modeling of the cerebral haemodynamics (Mandeville *et al* 1999, Buxton and Frank 1997, Buxton *et al* 1998, Friston *et al* 2000, Kong *et al* 2004, Zheng *et al* 2005). Similarly, it is also not appropriate to use the modified Grubb's exponent estimated here ($G' = 0.13$) to predict CBFV based on CBV measurement. As an example, linear regression with $\log(\text{CBV}/\text{CBV}_0)$ as the independent variable and $\log(\text{CBFV}/\text{CBFV}_0)$ as the dependent variable will result in a $\beta' = 3.9$ which is different from $1/G' (= 1/0.13 = 7.7)$.

Acknowledgments

The authors would like to thank Hamamatsu Photonics KK, the Wellcome Trust (grant no 075608) and the Engineering and Physical Sciences Research Council (grant no EP/G005036/1 and GR/N14248/01) for their support in this work, and Dr Ying Zheng of Sheffield University for the discussion of the balloon model. This work was undertaken at UCLH/UCL and partially funded by the Department of Health's National Institute for Health Research Centres funding. This study was in part funded by a donation in memory of Carolyn Margaret Jones.

References

- Aaslid R, Markwalder T-M and Nornes H 1982 Noninvasive transcranial Doppler ultrasound recording of flow velocity in basal cerebral arteries *J. Neurosurg.* **57** 769–74
- Al-Rawi P G, Smielewski P and Kirkpatrick P J 2001 Evaluation of a near-infrared spectrometer (NIRO 300) for the detection of intracranial oxygenation changes in the adult head *Stroke* **32** 2492–500
- Bishop C C, Powell S, Rutt D and Browse N L 1986 Transcranial Doppler measurement of middle cerebral artery blood flow velocity: a validation study *Stroke* **17** 913–5
- Boas D A, Strangman G, Culver J P, Hoge R D, Jaszewski G, Poldrack R A, Rosen B R and Mandeville J B 2003 Can the cerebral metabolic rate of oxygen be estimated with near-infrared spectroscopy? *Phys. Med. Biol.* **48** 2405–18
- Brauer P, Kochs E, Werner C, Bloom M, Policare R, Pentheny S, Yonas H, Kofke W A and am Esch J S 1998 Correlation of transcranial Doppler sonography mean flow velocity with cerebral blood flow in patients with intracranial pathology *J. Neurosurg. Anesthesiol.* **10** 80–5
- Buxton R B and Frank L R 1997 A model for the coupling between cerebral blood flow and oxygen metabolism during neural stimulation *J. Cereb. Blood Flow Metab.* **17** 64–72
- Buxton R B, Wong E C and Frank L R 1998 Dynamics of blood flow and oxygenation changes during brain activation: the balloon model *Magn. Reson. Med.* **39** 855–64

- Cenic A, Nabavi D G, Craen R A, Gelb A W and Lee T-Y 1999 Dynamic CT measurement of cerebral blood flow: a validation study *AJNR Am. J. Neuroradiol.* **20** 63–73
- Cheung C, Culver J P, Takahashi K, Greenberg J H and Yodh A G 2001 *In vivo* cerebrovascular measurement combining diffuse near-infrared absorption and correlation spectroscopies *Phys. Med. Biol.* **46** 2053–65
- Culver J P, Durduran T, Furuya T, Cheung C, Greenberg J H and Yodh A G 2003 Diffuse optical tomography of cerebral blood flow, oxygenation, and metabolism in rat during focal ischemia *J. Cereb. Blood Flow Metab.* **23** 911–24
- Dawson-Saunders B and Trapp R G 1994 *Basic & Clinical Biostatistics* (Connecticut: Appleton & Lange)
- Delpy D T and Cope M 1997 Quantification in tissue near-infrared spectroscopy *Phil. Trans. R. Soc. B* **352** 649–59
- Elwell C E, Springett R, Hillman E and Delpy D T 1999 Oscillations in cerebral haemodynamics—implications for functional activation studies *Adv. Exp. Med. Biol.* **471** 57–65
- Franceschini M A, Thaker S, Themelis G, Krishnamoorthy K K, Bortfeld H, Diamond S G, Boas D A, Arvin K and Grant P E 2007 Assessment of infant brain development with frequency-domain near-infrared spectroscopy *Pediatr. Res.* **61** 546–51
- Friston K J, Mechelli A, Turner R and Price C J 2000 Nonlinear responses in fMRI: the balloon model, Volterra kernels, and other hemodynamics *Neuroimage* **12** 466–77
- Grubb R L, Raichle M E, Eichling J O and Ter-Pogossian M M 1974 The effects of changes in PaCO₂ cerebral blood volume, blood flow and vascular mean transit time *Stroke* **5** 630–9
- Ito H, Kanno I, Ibaraki M, Hatazawa J and Miura S 2003 Changes in human cerebral blood flow and cerebral blood volume during hypercapnia and hypocapnia measured by positron emission tomography *J. Cereb. Blood Flow Metab.* **23** 665–70
- Jones M, Berwick J, Johnston D and Mayhew J 2001 Concurrent optical imaging spectroscopy and laser-Doppler flowmetry: the relationship between blood flow, oxygenation, and volume in rodent barrel cortex *Neuroimage* **13** 1002–15
- Koizumi H, Yamamoto T, Maki A, Yamashita Y, Sato H, Kawaguchi H and Ichikawa N 2003 Optical topography: practical problems and new applications *Appl. Opt.* **42** 3054–62
- Kong Y, Zheng Y, Johnston D, Martindale J, Jones M, Billings S and Mayhew J 2004 A model of the dynamic relationship between blood flow and volume changes during brain activation *J. Cereb. Blood Flow Metab.* **24** 1382–92
- Lee S-P, Duong T Q, Yang G, Iadecola C and Kim S-G 2001 Relative changes of cerebral arterial and venous blood volumes during increased cerebral blood flow: implications for BOLD fMRI *Magn. Reson. Med.* **45** 791–800
- Leung T S, Tisdall M M, Tachtsidis I, Smith M, Delpy D T and Elwell C E 2008 Cerebral tissue oxygen saturation calculated using low frequency haemoglobin oscillations measured by near infrared spectroscopy in adult ventilated patients *Adv. Exp. Med. Biol.* **614** 235–44
- Mandeville J B, Marota J J, Ayata C, Zaharchuk G, Moskowitz M A, Rosen B R and Weisskoff R M 1999 Evidence of a cerebrovascular postarteriole windkessel with delayed compliance *J. Cereb. Blood Flow Metab.* **19** 679–89
- Martin C G, Hansen T N, Goddard-Finegold J, LeBlanc A, Giesler M E and Smith S 1990 Prediction of brain blood flow using pulsed Doppler ultrasoundography in newborn lambs *J. Clin. Ultrasound* **18** 487–95
- Obrig H, Neufang M, Wenzel R, Kohl M, Steinbrink J, Einhaupl K and Villringer A 2000 Spontaneous low frequency oscillations of cerebral hemodynamics and metabolism in human adults *Neuroimage* **12** 623–39
- Panerai R B 1998 Assessment of cerebral pressure autoregulation in humans—a review of measurement methods *Physiol. Meas.* **19** 305–38
- Pindzola R R, Balzer J R, Nemoto E M, Golstein S and Yonas H 2001 Cerebralvascular reserve in patients with carotid occlusive disease assessed by stable Xenon-enhanced CT cerebral blood flow and transcranial Doppler *Stroke* **32** 1811–7
- Suzuki S, Takasaki S, Ozaki T and Kobayashi Y 1999 A tissue oxygenation monitor using NIR spatially resolved spectroscopy *Proc. SPIE* **3597** 582–92
- Ulrich P T, Becker T and Kempfski O S 1995 Correlation of cerebral blood flow and MCA flow velocity measured in healthy volunteers during acetazolamide and CO₂ stimulation *J. Neurosurg. Sci.* **129** 120–30
- Uludag K, Dubowitz D J, Yoder E J, Restom K, Liu T T and Buxton R B 2004 Coupling of cerebral blood flow and oxygen consumption during physiological activation and deactivation measured with fMRI *NeuroImage* **23** 148–55
- Vernieri F V, Tibuzzi F, Pasqualetti P, Rosato N, Passarelli F, Rossini P M and Silvestrini M 2004 Transcranial Doppler and near-infrared spectroscopy can evaluate the hemodynamic effect of carotid artery occlusion *Stroke* **35** 64–72
- Wu G, Luo F, Li Z, Zhao X and Li S 2002 Transient relationships among BOLD, CBV and CBF changes in rat brain as detected by functional MRI *Magn. Reson. Med.* **48** 987–93
- Zheng Y, Johnston D, Berwick J, Chen D, Billings S and Mayhew J 2005 A three-compartment model of the hemodynamic response and oxygen delivery to brain *NeuroImage* **28** 925–39